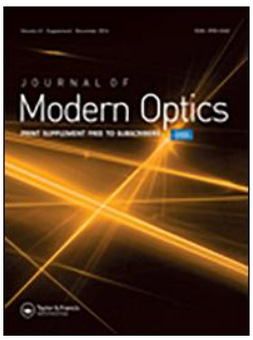

Journal of Modern Optics

ISSN: 0950-0340 (Print) 1362-3044 (Online) Journal homepage: https://www.tandfonline.com/loi/tmop20

Measurement of planar refractive index profiles with rapid variations in glass using interferometry and total variation regularized differentiation

R. Oven

To cite this article: R. Oven (2015) Measurement of planar refractive index profiles with rapid variations in glass using interferometry and total variation regularized differentiation, Journal of Modern Optics, 62:sup2, S53-S60, DOI: 10.1080/09500340.2015.1083130

To link to this article: https://doi.org/10.1080/09500340.2015.1083130

Journal of Modern Optics, 2015
Vol. 62, No. S2, S53–S60, http://dx.doi.org/10.1080/09500340.2015.1083130

Taylor & Francis
Taylor & Francis Group

Measurement of planar refractive index profiles with rapid variations in glass using interferometry and total variation regularized differentiation

R. Oven*

School of Engineering and Digital Arts, The University of Kent, Canterbury, UK

(*Received 27 March 2015; accepted 10 August 2015*)

Planar refractive index profiles with rapid variations, formed in glass, are measured with interferometry. This involves forming a bevel in the glass and orientating the fringe pattern to be normal to the bevel edge. The index profile is determined by differentiation of the phase function of the fringe pattern. The differentiation has been performed using the total variation regularization method in order to preserve rapid changes in the derivative. This new approach avoids the necessity of filtering, in order to reduce noise, in the direction perpendicular to the bevel, which would otherwise smooth out the rapid index changes. The method is assessed using a model refractive index profile that contains an index gradient of 0.24 μm^{-1} and is then applied practically to measure the refractive index profile of electrically poled BK7 glass. The new approach allows the sharp transition in the index between poled and unpoled glass to be observed as well as the accumulation of potassium ions beyond the poled glass region.

Keywords: fringe pattern analysis; total variation regularization differentiation; poled glass; refractive index profile

1. Introduction

There are many ways to measure the refractive index profile in a graded index sample. These include ellipsometry using multiple angle data [1], mode measurements mediated with a prism coupler (for both guided and leaky modes) [2–4], reflectance analysis [5,6] and numerous interferometric methods [7–13]. Each method has advantages and disadvantages. For example, ellipsometry and mode analysis methods require no sample preparation and are nondestructive. They are, however, only applicable to index profiles that are planar. If the sample supports both guided and leaky modes, then the mode measurement method relies on having a model for the index profile whose parameters require adjustment to fit the experimental data [2,3]. Hence, some a priori knowledge of the index profile is required. If the sample is known to support only guided modes, then a smooth monotonically decreasing index profile can be deduced without further assumptions [4]. Reflectance measurements are not limited to planar index profiles but require careful sample preparation and are sensitive only to large index differences [5,6]. Interferometric measurements on cross sections of samples require careful sample preparation and are limited to the analysis of index profiles that are deep due to the magnification of the optical system [8]. On the other hand, they can measure two-dimensional index profiles. Some other interferometric methods, although they are nondestructive, require a model for the index profile and can only provide information on planar index profiles [9].

A number of studies have reported on the measurement of refractive index profiles formed in glass using interferometry with a bevelled sample [10–13]. In these studies, depth information is imparted onto the interferogram by analysing the sample, in which a bevel has been formed in the surface by polishing. The bevel cuts through the index profile, thereby transforming depth information into lateral information. The method has been used to obtain refractive index profiles of both planar and two-dimensional form made by ion exchange processes in glass [10–13]. Clearly, the method is time-consuming and partially destructive but it is not necessary to assume a model index profile since the refractive index profile is proportional to the phase derivative of the interference pattern in the direction perpendicular to the bevel edge. In a number of studies, the interferometer fringes have been orientated with the fringes parallel to the bevel for the analysis of channel waveguides with two-dimensional refractive index profiles, [12,13]. This fringe orientation has also been used for the analysis of planar waveguides [11].

Various algorithms have been used to analyse the fringe data produced by this technique including Fourier fringe analysis [11], a regularization technique [12] and wavelet transforms [13]. In the Fourier and the regularization technique, the phase is first obtained and is then numerically differentiated, whilst in the wavelet

*Email: R.Oven@kent.ac.uk

transform method, the phase derivative is obtained directly. The current author has also used a windowed Fourier transform method [14] to achieve a similar analysis. Irrespective of what technique is used, with the above analysis methods, there is inevitably some degree of filtering (averaging) to the fringe data occurring in the direction perpendicular to the bevel edge. The extent of the filtering required depends on the level of the noise that will inevitably be present in the interferometer image. In the Fourier method, a filter is used to extract the appropriate Fourier component [15]. In the regularization technique, the phase is assumed to vary linearly over a window of the order of a fringe period and the regularization can impose further smoothing [12]. In the wavelet technique and the windowed Fourier transform method, the phase derivative is determined by the fringe pattern encompassed within a Gaussian window function. These will all tend to smooth out any rapid variations in the index profile. This thus highlights a potential disadvantage of this method in analysing samples with rapid changes in the refractive index profile; they can be smoothed out due to the filtering processes. This can be partially overcome by reducing the strength of any regularization smoothing in regions of the profile where a rapid index variation is known a priori at the expense of a reduction in the filtering effect [12,13].

In this study, we investigate the use of a different numerical approach that overcomes the above problem. In the method, the fringes are rotated by 90° so they are perpendicular to the bevel edge in the unbevelled part of the glass. This means that for a planar index profile, along a line of the image parallel to the bevel edge, the phase of the interferogram is almost a constant. This implies that it is not necessary to choose a phase analysis technique with a small filter window in that direction. However, in order to obtain the index profile, it is still necessary to determine the phase derivative in the bevelled region in the direction perpendicular to the bevel edge. This then necessitates differentiation of the phase data, which will inevitably contain noise. However, smoothing coupled with normal finite difference differentiation will again result in a recovered index profile where the rapid transitions are smoothed out. Hence, in this study, we investigate the use of a total variation regularization differentiation (TVRD) algorithm [16]. This algorithm has been applied in numerous fields of study other than interferometry and has been shown to be effective at recovering the derivative of a function even in the presence of noise but it preserves rapid variations in the derivative. Here, we apply the TVRD algorithm for the first time, to our knowledge, in the field of interferometry. For our application, it hence allows us to recover rapid changes in the refractive index profile that are not possible using the previous approaches. A total variation regularization technique for the recovery of phase functions has recently been reported [17]. However, this is applicable to the case where the phase function itself is expected to have discontinuities or rapid changes in them. In our study, rapid changes in the phase derivative are of interest.

In Section 2 of this study, the interferometer method is outlined in more detail. In Section 3, the TVRD method is summarized. In Section 4, the recovery of an index profile from noiseless and noisy model fringe data using the TVRD algorithm is compared with that recovered using conventional finite difference differentiation. Finally, in Section 5, the TVRD algorithm is used to analyse practical fringe data obtained by analysing electrically poled BK7 glass.

2. Interferometer measurements

The measurement technique involves polishing a shallow bevel (typically 2°–8° depending on the expected depth of the index profile) in the glass surface, which passes through the index profile. The sample together with index matching oil is placed on a reflective optical flat in one arm of an interferometer [12,13]. Due to the reflective optical flat, the light passes twice through the sample and then interferes with a reference beam. The fringes are orientated to be perpendicular to the bevel edge as shown in Figure 1. With this orientation, the influence of the index profile on the fringes can clearly be observed. Hence, moving from top to bottom of Figure 1, the fringes change orientation at line A–A due to the start of the bevel. Near line B–B, the fringes change orientation again due to the end of the index profile layer. Well beyond line B–B, the fringe orientation is due to the bevelling continuing into the bulk of the glass. The index depth profile $n(z)$ is related to the gradient of the phase, ϕ, of the interferometer image by

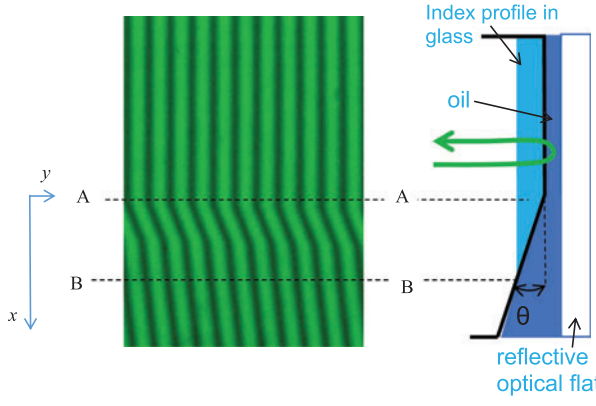

Figure 1. Interferometer image and details of arrangement in sample arm of interferometer showing bevelled sample, index matching fluid and reflective optical flat. (The colour version of this figure is included in the online version of the journal.)

$$n = n_0 \quad x<0$$

$$n(z = x\tan\theta) = n_0 - \frac{\lambda}{4\pi\tan\theta}\frac{\mathrm{d}\phi}{\mathrm{d}x} \quad x > 0 \qquad (1)$$

where x is the coordinate defined in Figure 1 and is measured from the start of the bevel, θ is the bevel angle and n_0 is the refractive index of the oil. The wavelength of light λ used for the measurements is 546 nm. The bevel angle was measured with a Dektak 6 M surface profiler.

3. Total variation regularization differentiation

The TVRD algorithm has been applied to numerical data from a number of research fields [15]. Here, we use the algorithm to obtain the phase derivative $\phi' = \mathrm{d}\phi/\mathrm{d}x$ from the phase function ϕ. The TVRD algorithm is based on minimizing a functional F [16]. For our application, we write it in terms of ϕ and its derivate as

$$F(\phi') = \frac{1}{2}\int_0^L |A\phi' - \phi|^2 \mathrm{d}x + \alpha\int_0^L |\phi'|\mathrm{d}x \qquad (2)$$

In this expression, $A\ \phi'$ is the integral $\int_0^x \phi'\mathrm{d}x$. The first term in Equation (2) is the data term. The second term is the sum of the total variation in the phase derivative. Minimizing F with the second term included results in a solution that contains less noise since noisy solutions have large total variation. The relative importance of the total variation term is determined by the regularization parameter α. Minimizing F amounts to finding the solution to the following Euler–Lagrange equation [16]

$$0 = \alpha\frac{\mathrm{d}}{\mathrm{d}x}\frac{\phi'}{|\phi'|} - A^T(A\phi' - \phi) \qquad (3)$$

where $A^T v(x) = \int_x^L v\mathrm{d}x$. Details on the implementation of the algorithm to solve Equation (3) are given elsewhere [16].

4. Analysis using model data

In order to assess the effectiveness of the algorithm, two artificial fringe patterns are generated based on a model refractive index profile with sharp transitions. We choose an index profile of the form of a Fermi function

$$n(z) = n_{\mathrm{sub}} - \frac{\Delta n}{1 + \exp\left(\frac{z-d}{a}\right)} \qquad (4)$$

where $n_{\mathrm{sub}} = 1.5187$, $\Delta n = 0.05$, $d = 3$ μm and $a = 0.04$ μm. This is used to generate a model fringe pattern for a 4° bevelled glass substrate and an index oil of 1.54. The amplitude of the fringe pattern is unity and has a period of 30 pixels. For one of the fringe patterns, Gaussian noise with a standard deviation of 0.4 is added. A value of $a = 0.04$ μm corresponds to an average transition width from $n = n_{\mathrm{sub}} - 0.9\Delta n$ to $n = n_{\mathrm{sub}} - 0.1\Delta n$ of 0.17 μm; hence, the average refractive index gradient of the model index profile is 0.24 $\mu\mathrm{m}^{-1}$.

The phase of the model fringe patterns is determined row by row (y coordinate, see Figure 1) using a synchronous detection algorithm [18] followed by smoothing and differentiation in the x direction or just application of the TVRD algorithm. Averaging can be done over the y coordinate to further reduce the fluctuations due to noise. This is important for those profiles not recovered by the TVRD algorithm. We first consider the recovery of the index profile from these patterns by smoothing with a moving average filter of 20 pixels width in the x direction with standard numerical differentiation. Figures 2 and 3 show the recovered profiles using this approach in comparison with the original profile in Figure 2 from the noiseless fringe pattern and in Figure 3 using the fringe pattern with noise. The index profile of Figure 3 is clearly still affected by the noise in the fringe pattern and suggests that more smoothing is required. But the recovered profile in Figure 3, and more clearly in Figure 2, shows that the transitions in the index profile are already being smeared out by this degree of smoothing. 20 pixels corresponds to a spread in depth $\Delta z = 20 \cdot p \cdot \tan(\theta)$ where p is the magnified pixel size in μm. This gives $\Delta z \sim 0.5$ μm which is greater than the average transition width of 0.17 μm.

For comparison, Figures 4 and 5 show the index profile recovered using the TVRD algorithm with $\alpha = 5$. Figure 4 is obtained from the noiseless fringe pattern, and Figure 5 is obtained from the fringe pattern with noise. It can be seen from Figure 4 that the TVRD algorithm recovers the index profile with good accuracy including the transitions whilst Figure 5 shows that the fluctuations due to the noise are greatly suppressed. Numerically, the RMS error between the model and recovered profile is 0.0035 for the profiles in Figure 4 and has only increased to 0.0037 for the profiles in Figure 5.

Figure 6 shows the recovered index profiles for various values of the regularization parameter α using the fringe pattern with noise. It can be seen that small values of α result in little smoothing of the noise whilst very large values of α overly smooth the recovered index profile and sharp transitions in the index profile are eventually lost with the TVRD algorithm. It can also be seen from Figure 6 that very large values of α also result in a loss of contrast (i.e. a reduction in the magnitude of the transition in the index). This loss of contrast in the derivative for large α is a known effect of the TVRD algorithm in the presence of noise and can be reduced using as small a value of α as possible consistent with the required noise reduction [16].

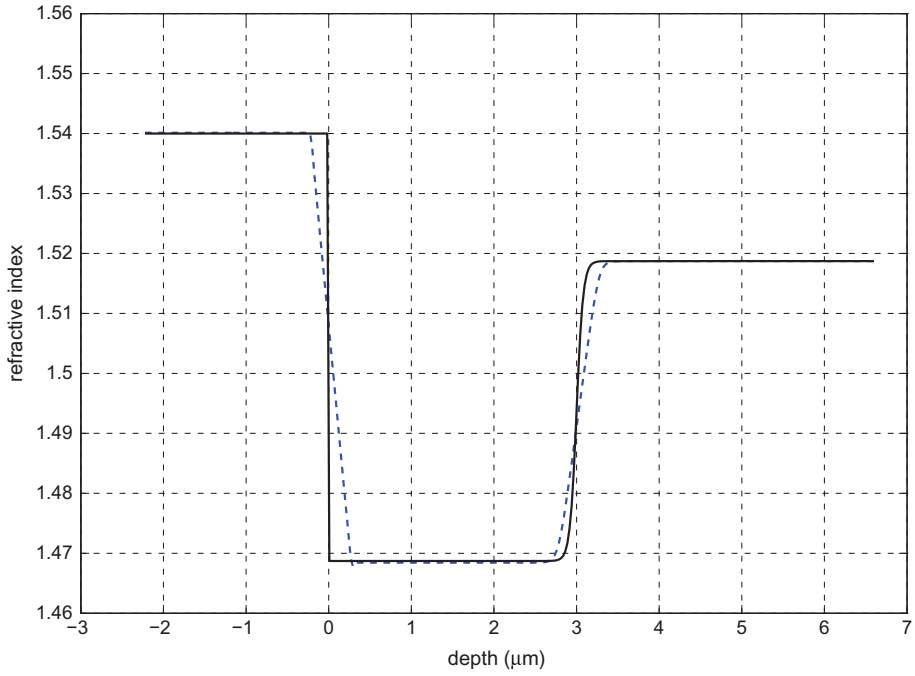

Figure 2. (Solid) model index profile. (Dash) index profile recovered using smoothing and ordinary differentiation from model fringe data with no noise. (The colour version of this figure is included in the online version of the journal.)

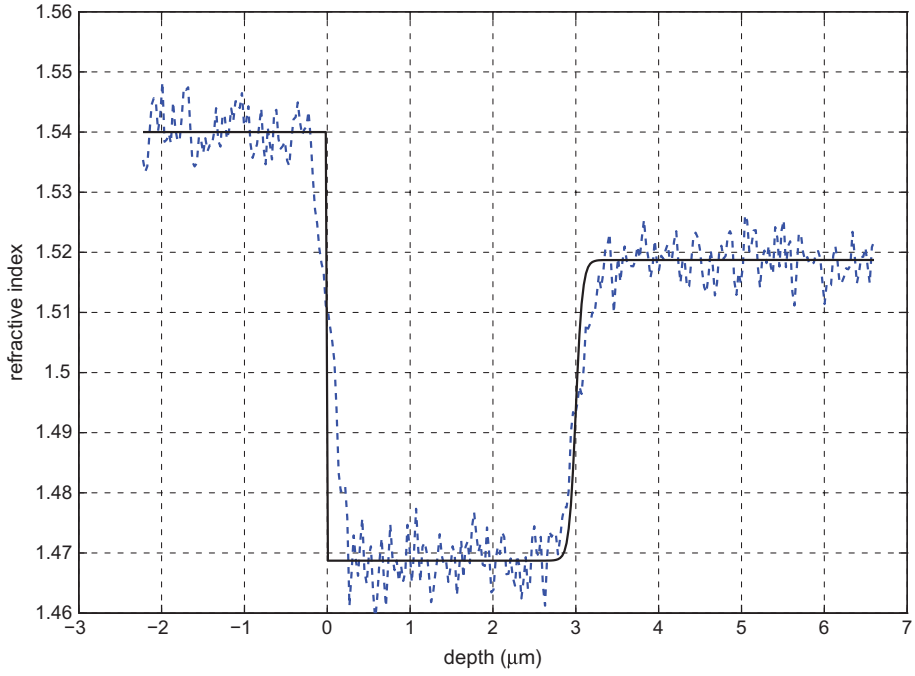

Figure 3. (Solid) model index profile. (Dash) index profile recovered using smoothing and ordinary differentiation from model fringe data with noise. (The colour version of this figure is included in the online version of the journal.)

5. Measurements on poled glass

The effectiveness of the bevel method coupled with the TVRD algorithm is demonstrated by investigating a sample of BK7 glass that has been electrically poled at ~2 kV at 261 °C. The glass is poled using graphite electrodes in air. The poling process forms a region of glass

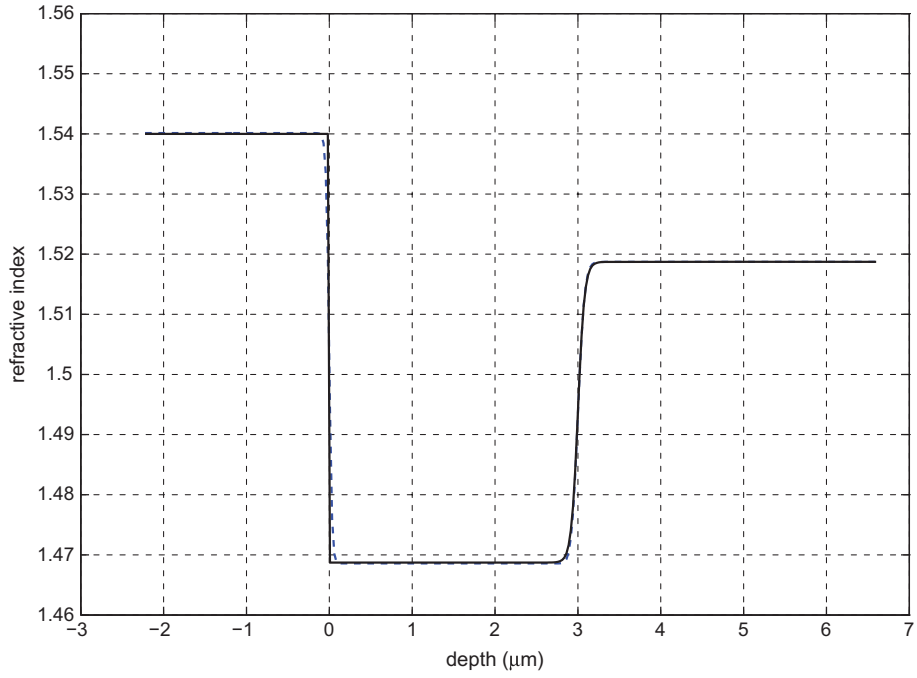

Figure 4. (Solid) model index profile. (Dash) index profile recovered using TVRD from model fringe data with no noise. Regularization parameter $\alpha = 5$. (The colour version of this figure is included in the online version of the journal.)

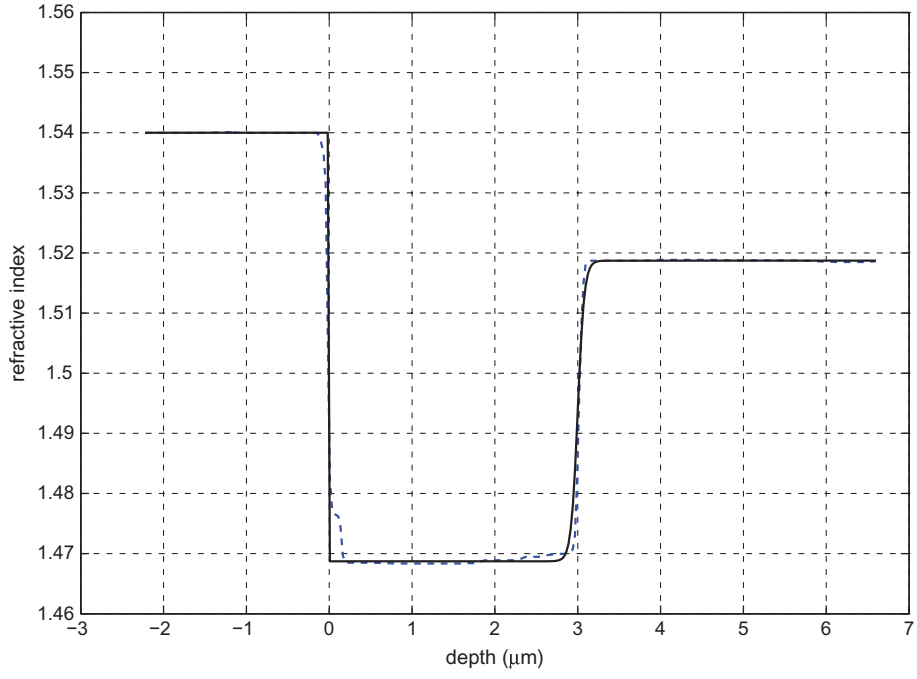

Figure 5. (Solid) model index profile. (Dash) index profile recovered using TVRD from model fringe data with noise. Regularization parameter $\alpha = 5$. (The colour version of this figure is included in the online version of the journal.)

below the anode that is depleted of mobile Na^+ and K^+ ions and hence reduces the refractive index [19–21]. Based on ion transport models of the process, a rapid change in Na^+ and K^+ ion concentrations is to be expected at a depth corresponding to the boundary between the depleted and undepleted glass [22]. Hence,

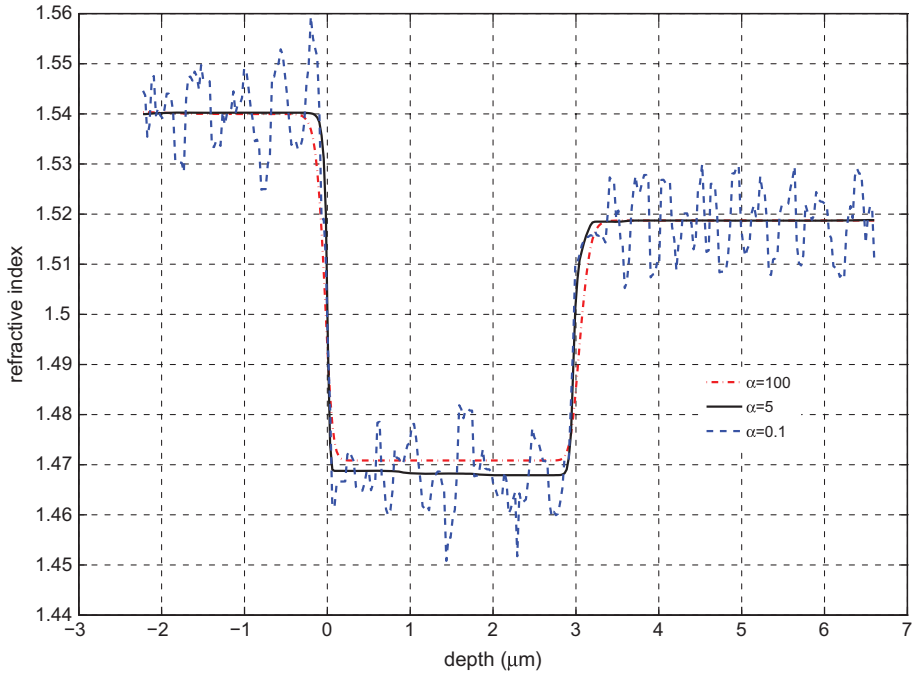

Figure 6. Index profiles recovered using TVRD from model fringe data with noise. Dash, $\alpha = 0.1$; solid $\alpha = 5$; dash-dot $\alpha = 100$. (The colour version of this figure is included in the online version of the journal.)

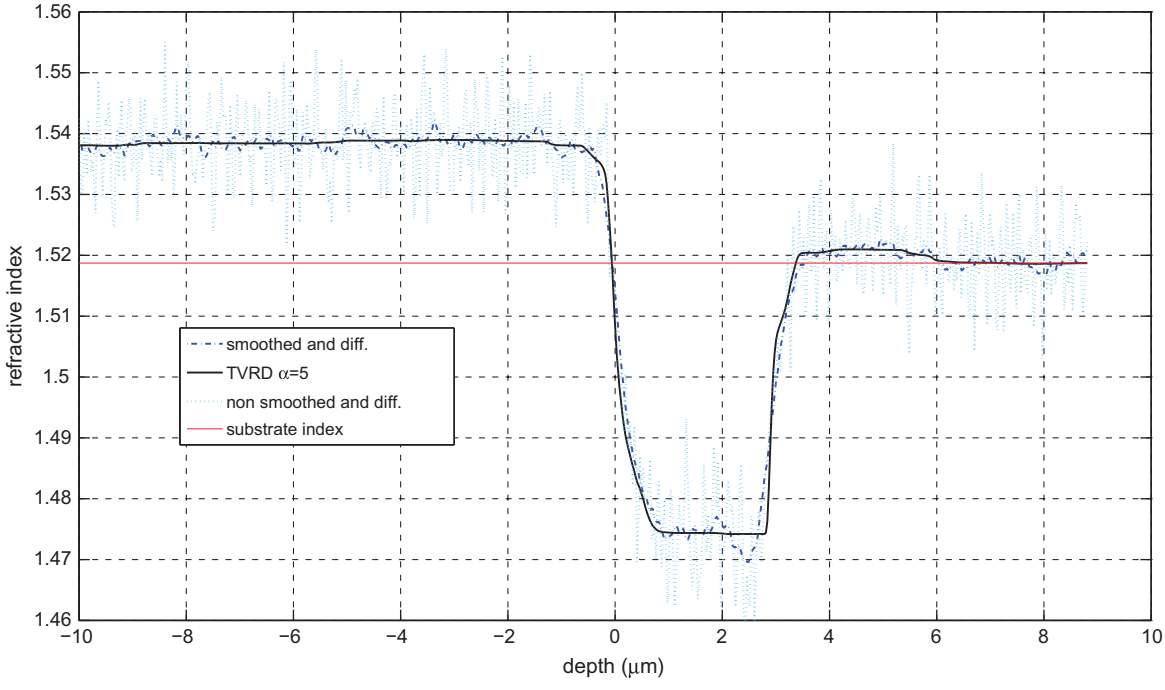

Figure 7. Poled glass index profile recovered using TVRD. $\alpha = 5$. (Dash-dot) unsmoothed and ordinary differentiation; (Dash) smoothed and ordinary differentiation; (Solid) using TVRD with $\alpha = 5$. Horizontal line is bulk refractive index. (The colour version of this figure is included in the online version of the journal.)

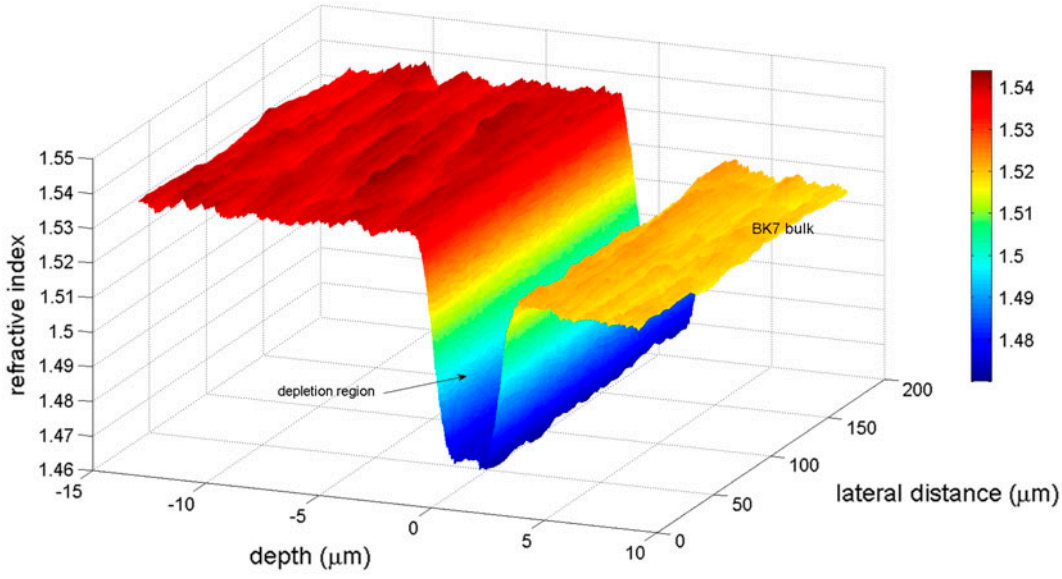

Figure 8. Poled glass refractive index surface recovered using smoothing with normal differentiation. (The colour version of this figure is included in the online version of the journal.)

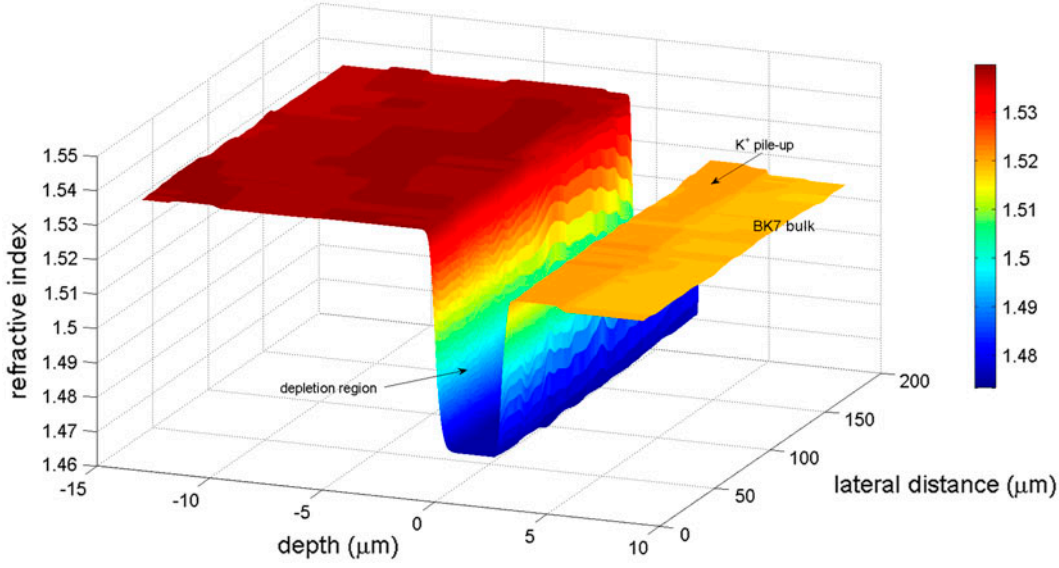

Figure 9. Poled glass refractive index surface recovered using TVRD. (The colour version of this figure is included in the online version of the journal.)

a rapid change in the refractive index at that depth is to be expected. Figure 7 shows a graph of the index profile extracted using normal differentiation on the unsmoothed data, smoothing and normal differentiation and that obtained using the TVRD algorithm. It can be seen that the refractive index in the poled glass region is ~1.475, and the refractive index changes rapidly between the depleted glass and the bulk of the sample. The reduction in refractive index observed between the bulk unpoled glass and the depletion region $\Delta n \sim 0.045$ is larger than that estimated for poled V073 glass $\Delta n \sim 0.02$, which is evidently similar in composition to BK7 [21]. From Figure 7, it is also possible to observe a small (~0.0023) increase in refractive index above the substrate index immediately under the poled glass region in the unpoled glass. This can be attributed to the pile-up of K^+ ions that are present in BK7 glass. They are removed from the poled glass region and accumulate just beyond the

poled region due to their lower mobility in comparison with the sodium ions [19,20]. K^+ ions have a larger polarizability than Na^+ ions and also cause stress-induced index changes resulting in an increase in the refractive index [19,23]. The index profile due to the K^+ ions can be observed to be approximately step-like in shape which is consistent with field assisted diffusion [22].

The near surface profile is strongly influenced by the quality of the bevel. For the sample shown in Figure 7, the transition in the bevel was measured with a surface profiler and extends over a distance x, as defined in Figure 1, of 4 μm. This converts to a depth range, z, in Figure 7 of ~0.3 μm. Hence, although there is some evidence in Figure 7 of a slope in the index profile within the glass near the surface, the data are distorted by the bevel profile. Figures 8 and 9 show the complete refractive index surfaces for the same sample recovered using smoothing with normal numerical differentiation and by TVRD, respectively. The transitions in refractive index are sharper in the profile recovered using TVRD. The increase in refractive index due to the accumulation of K^+ ions is hardly discernible in the profile obtained with smoothing and normal differentiation (Figure 8), but can clearly be observed in the surface obtained by TVRD (Figure 9).

6. Conclusions

Planar refractive index depth profiles in glass with rapid variations in refractive index have been measured using an interferometric method. This involves forming a bevel in the glass and orientating the fringe pattern to be normal to the bevel edge. The differentiation of the phase function has been performed using the TVRD method in order to reduce the effects of noise but preserve the rapid transitions in the refractive index. This new approach has allowed us to measure the refractive index profile of electrically poled BK7 glass and observe the rapid transition in refractive index between the poled and unpoled glass. The region of glass depleted of Na^+ and K^+ ions is found to have a refractive index of ~1.475. In addition, the method has allowed the observation of the index change caused by the accumulation of K^+ ions below the poled glass region.

Acknowledgements

The author thanks the Faculty of Sciences, University of Kent, for partial funding of this research.

Disclosure statement

No potential conflict of interest was reported by the author.

References

[1] Tonova, D.; Paneva, A.; Pantchev, B. *Opt. Commun.* **1998,** *150,* 121–125.
[2] Townsend, P.D.; Chandler, P.J.; Zhang, L. *Optical Effects of Ion Implantation*; Cambridge Studies in Modern Optics; Cambridge University Press: Cambridge, 1994. ISBN 0-521-39430-9.
[3] Cardin, J.; Leduc, D. *Appl. Opt.* **2008,** *47,* 894–900.
[4] Chiang, K.S. *J. Lightwave Technol.* **1985,** *3,* 385–391.
[5] Lilienhof, H.J.; Voges, E.; Ritter, D.; Pantschew, B. *IEEE J. Quantum Electron*. **1982,** *18,* 1877–1883.
[6] Steffen, J.; Neyer, A.; Voges, E.; Hecking, N. *Appl. Opt.* **1990,** *29,* 4468–4472.
[7] Goldberg, L. *Appl. Opt.* **1981,** *20,* 3580–3588.
[8] Mrozek, P.; Mrozek, E.; Lukaszewicz, T. *Appl. Opt.* **2006,** *45,* 756–763.
[9] Fazio, E.; Ramadan, W.A.; Bertolotti, M. *Opt. Lett.* **1996,** *21,* 1238–1240.
[10] Sochacka, M.; Lopez Lago, E.; Jaroszewicz, Z. *Appl. Opt.* **1994,** *33,* 3342–3347.
[11] Darudi, A.; Hosseini, S.M.R.S. *Opt. Lasers Eng.* **2008,** *47,* 133–138.
[12] Oven, R. *Appl. Opt.* **2009,** *48,* 5704–5712.
[13] Oven, R. *Appl. Opt.* **2010,** *49,* 4228–4236.
[14] Kemao, Q. *Opt. Lasers Eng.* **2007,** *45,* 304–317.
[15] Takeda, M.; Ina, H.; Kobayashi, S. *J. Opt. Soc. Am.* **1982,** *72,* 156–160.
[16] Chartrand, R. *ISRN Appl. Mech*., **2011,** *2011,* 164564-1–164564-11. DOI: 10.5402/2011/164564.
[17] Legarda-Saenz, R.; Brito-Loeza, C.; Espinosa-Romero, A. *Appl. Opt.* **2014,** *53,* 2297–2301.
[18] Yañez-Mendiola, J.; Servín, M.; Malacara-Hernández, D. *Opt. Commun.* **2000,** *178,* 291–296.
[19] Brennand, A.L.R.; Wilkinson, J.S. *Opt. Lett.* **2002,** *27,* 906–908.
[20] An, H.; Fleming, S. Appl. Phys. Lett. **2006,** *89,* 181111-1–181111-3.
[21] Lipovskii, A.A.; Rusan, V.V.; Tagantsev, D.K. *Solid State Ionics* **2010,** *181,* 849–855.
[22] Petrov, M.I.; Lepen'kin, Y.A.; Lipovskii, A.A. *J. Appl. Phys.* **2012,** *112,* 043101.
[23] Miliou, A.N.; Srivastava, R.; Ramaswamy, R.V. *Appl. Opt.* **1991,** *30,* 674–681.